Neuron, Vol. 31, 477–485, August 16, 2001, Copyright ©2001 by Cell Press

Synchronous Activity of Inhibitory Networks in Neocortex Requires Electrical Synapses Containing Connexin36

Michael R. Deans,[1,4] Jay R. Gibson,[2,4] Caterina Sellitto,[1] Barry W. Connors,[2] and David L. Paul[1,3]
[1] Department of Neurobiology
Harvard Medical School
Boston, Massachusetts 02115
[2] Department of Neuroscience
Brown University
Providence, Rhode Island 02912

Summary

Inhibitory interneurons often generate synchronous activity as an emergent property of their interconnections. To determine the role of electrical synapses in such activity, we constructed mice expressing histochemical reporters in place of the gap junction protein Cx36. Localization of the reporter with somatostatin and parvalbumin suggested that Cx36 was expressed largely by interneurons. Electrical synapses were common among cortical interneurons in controls but were nearly absent in knockouts. A metabotropic glutamate receptor agonist excited LTS interneurons, generating rhythmic inhibitory potentials in surrounding neurons of both wild-type and knockout animals. However, the synchrony of these rhythms was weaker and more spatially restricted in the knockout. We conclude that electrical synapses containing Cx36 are critical for the generation of widespread, synchronous inhibitory activity.

Introduction

The cerebral cortex generates a variety of synchronized, often rhythmic patterns of activity that vary with behavioral state (Steriade, 1997). The cellular mechanisms underlying most of these patterns are unknown. One possibility is that correlated synaptic inhibition coordinates the timing of spikes in large cortical circuits (Buzsaki and Chrobak, 1995; Lytton and Sejnowski, 1991). This implies that networks of inhibitory interneurons can generate synchronized spiking, and studies both in vitro (Benardo, 1997; Michelson and Wong, 1994; Whittington et al., 1995) and in vivo (Bragin et al., 1995; Swadlow et al., 1998) suggest that this may be true under certain conditions. Synchronous inhibition is likely to be an emergent property of synaptic interactions within networks of interneurons (Jefferys et al., 1996). Recent work in the neocortex has shown that both the fast spiking (FS) (Galarreta and Hestrin, 1999; Gibson et al., 1999; Tamas et al., 2000) and the low threshold spiking (LTS) types of inhibitory interneurons are connected by electrical synapses (Gibson et al., 1999).

In principle, either chemical or electrical synapses could synchronize inhibitory cells. Indeed, FS cells are frequently interconnected by chemical inhibitory synapses (Galarreta and Hestrin, 1999; Tamas et al., 2000), but electrical synapses may be essential for coordinating the activity of at least some interneurons. In neocortical slices, the LTS interneurons generate highly synchronized patterns of either rhythmic or irregular spiking when activated by metabotropic glutamate or acetylcholine receptor agonists (Beierlein et al., 2000). Synchronous LTS firing in turn produces well-correlated patterns of inhibition in the local neural circuit of FS interneurons and excitatory neurons (i.e., regular spiking, or RS, cells). It seems likely that electrical synapses are critically necessary for coordinating the activity of LTS interneurons under experimental conditions for the following reasons (Beierlein et al., 2000; Gibson et al., 1999). First, the membrane potentials of LTS cells remain highly synchronized even when fast chemical synapses and action potentials are blocked. Second, LTS cells form electrical synapses almost exclusively with other LTS cells. Finally, chemical synapses between LTS cells are sparse.

Electrical synapses, or neuronal gap junctions, are composed of intercellular channels which span the plasma membranes of adjoining cells and directly connect their cytoplasms. In vertebrates, these channels are encoded by the connexin (Cx) family of genes (White and Paul, 1999), which contains at least 16 different members. Connexin-based channels are permeable to inorganic ions as well as to small molecules ($<$1000 Da), and thus couple cells both electrically and metabolically. Electrical coupling occurs in a wide variety of neurons in the vertebrate central nervous system (for review see Bennett [1997]). Transcripts for several Cx genes have been reported in rodent brain, but the identities of the neuronal connexins have not been completely established. Only Cx36 has been unequivocally identified at ultrastructurally defined neuronal gap junctions (Rash et al., 2000). In addition, Venance et al. (2000) have demonstrated the presence of Cx36 transcript in electrically coupled interneurons of the neocortex and hippocampus by single-cell RT-PCR. Thus, Cx36 is likely to be a component of electrical synapses between cortical interneurons.

To explore the role of interneuronal electrical synapses in the generation of synchronous and rhythmic activity in the neocortex, we constructed mice expressing histochemical reporters in place of Cx36. In the neocortex, Cx36 appeared to be expressed largely by interneurons. Loss of Cx36 was correlated with a near-total loss of electrical coupling between LTS cells and between FS cells while chemical synapses formed by these cells were normal. A metabotropic glutamate receptor agonist excited LTS interneurons, generating rhythmic inhibitory potentials in surrounding neurons of both wild-type and knockout animals. In the knockout animals, however, the synchrony of rhythms was far weaker and much more spatially restricted.

Results

Targeting the Cx36 Gene

Cx36 coding sequences were replaced with a bicistronic cassette containing two reporter genes; β-galactosi-

[3] Correspondence: dpaul@hms.harvard.edu
[4] These authors contributed equally to this work.

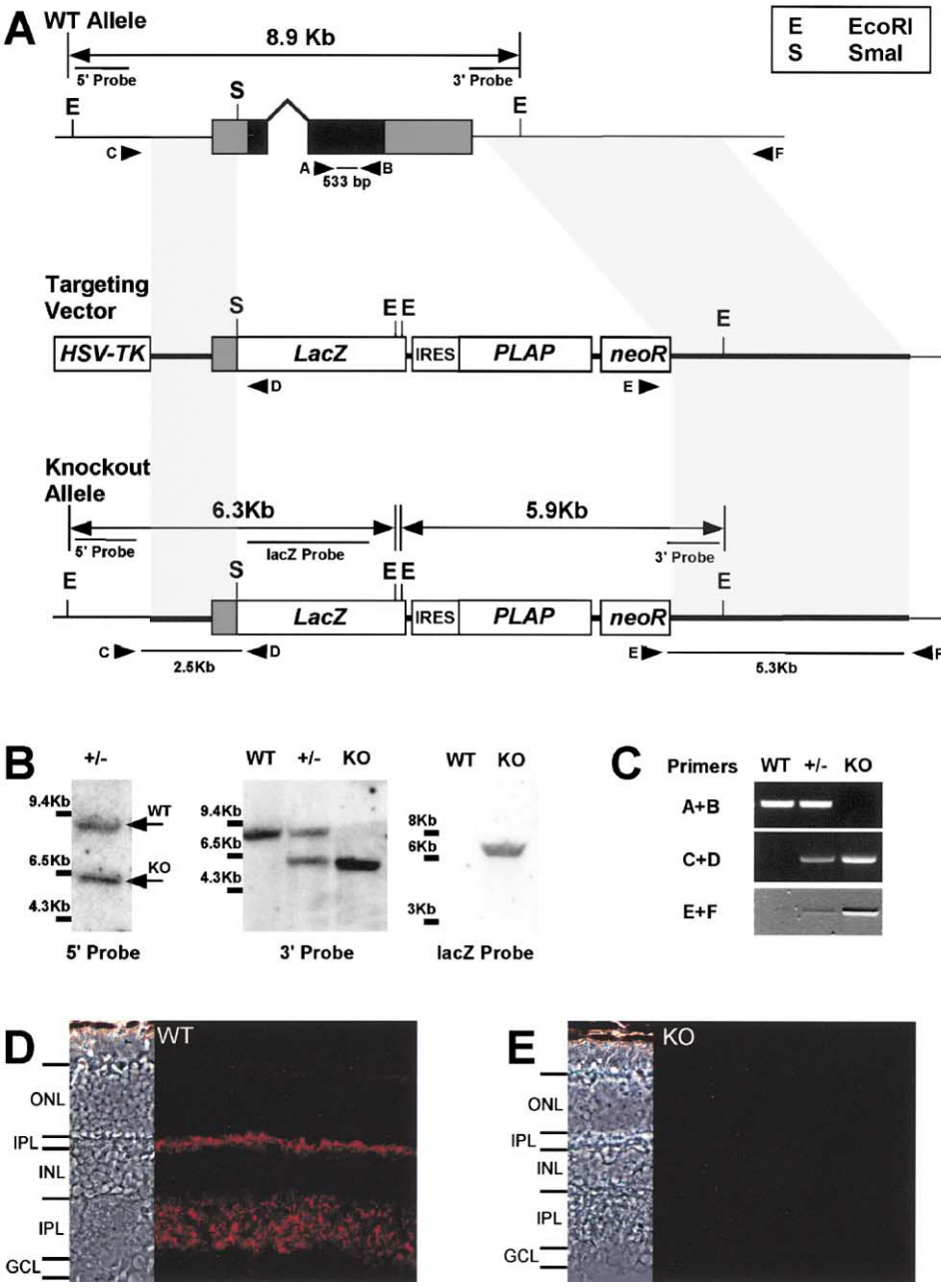

Figure 1. Targeting the Cx36 Gene

(A) Structure of wild-type (WT) and mutant alleles and targeting vector. Cx36 coding region was replaced with a bicistronic reporter cassette containing LacZ and IRES-PLAP. The 5′ homology region was supplied by a 2 kb Bgl2/Sma1 fragment, placing the start codon of β-galactosidase 71 bp upstream of the Cx36 start in the Cx36 5′ UTR.

(B and C) Analysis of homologous recombination. 5′ recombination was verified by Southern blot using a probe outside the targeting construct and confirmed using a LacZ probe. Because flanking 3′ probes were unavailable, 3′ recombination was assessed using an internal probe (B), then verified by PCR using a 5′ neo primer and a 3′ primer external to the targeting construct (C). To verify the loss of Cx36 protein, frozen sections of WT and knockout (KO) retina were stained with anti-Cx36 antibodies.

(D) WT retina exhibited punctate or macular staining confined to the plexiform layers, consistent with the known locations of gap junctions between retinal neurons.

(E) No signal above background was evident in KO retina.

dase (β-gal) and placental alkaline phosphatase (PLAP) (Figures 1A, 1B, and 1C). Translation of PLAP was driven by an internal ribosome entry site (IRES). In interneurons, only β-gal was expressed at levels sufficient for histological detection. Cx36 knockout animals were viable, fertile, and did not display gross anatomic or motor defects (data not shown). Loss of Cx36 expression in homozygotes was verified by immunostaining frozen sections of retina. For this demonstration, the principal advantages of the retina over the brain are the restriction of

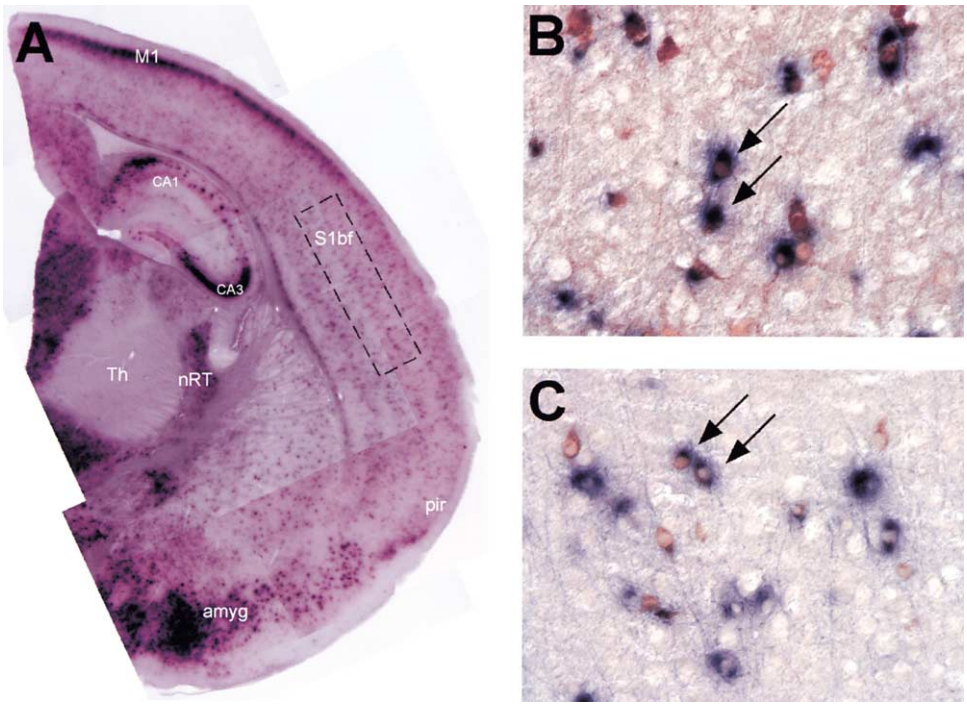

Figure 2. Cx36 Is Expressed in Many Areas of the CNS

(A) In low magnification view, β-gal reaction product is evident in many brain regions. The patterns of expression were similar if not identical in homo- and heterozygote specimens. The box encloses an area of somatosensory cortex where electrophysiological recordings were performed. M1, primary motor cortex; S1bf, barrel cortex; pir, piriform cortex; CA1/CA3, hippocampus; Th, thalamic nuclei; nRT, nucleus reticularis; amyg, amygdaloid nuclei.

(B and C) Interneuron marker expression in a region corresponding to box in (A). Frozen sections were histochemically labeled for β-gal (blue cells) then immunolabeled (brown cells) for either parvalbumin (B) or somatostatin (C). Arrows indicate examples of double positive cells. Most if not all Cx36-expressing cells in layer 4 were interneurons by the criteria of parvalbumin or somatostatin expression.

electrical synapses to anatomically distinct locations, the inner and outer plexiform layers (Raviola and Gilula, 1975; Raviola and Raviola, 1982), and the fact that Cx36 is particularly abundant (Sohl et al., 1998). While wild-type retinae exhibited strong punctate staining in those regions (Figure 1D), no signal was detected in Cx36 knockout retinae (Figure 1E).

Cx36 Marker Is Expressed Largely by Interneurons

The distribution of the β-gal reporter was determined histochemically in brain sections. The micrograph in Figure 2A displays a low magnification view of a 200 μM vibratome section from a postnatal day 15 (P15) knockout brain. The age of the specimen and the oblique orientation of the section is the same as that used for electrophysiological characterization. This orientation maintains some of the connections between thalamic relay nuclei and somatosensory cortex (Agmon and Connors, 1991). In neocortex, staining was evident in all layers where neuronal cell bodies were located, although the intensity depended on both the specific layer and the cortical area. For example, upper layer staining was modest in piriform cortex but increased dorsally to very high levels in primary motor and cingulate areas. In contrast, staining was virtually absent in thalamic nuclei with the exception of the nucleus reticularis. In the hippocampus, strong expression was observed in the pyramidal layer of CA3 but not CA1. In addition, cell bodies scattered in the strata oriens and radiatum were frequently labeled. In CA3, it was not possible to rule out expression by pyramidal cells, but in CA1 and the nonpyramidal areas the pattern of labeling was very similar to the distribution of GABAergic neurons. Similarly, the pattern of reporter expression in the dentate gyrus, neostriatum, and cerebellum (data not shown) corresponded well with the distribution of interneurons. Significant expression was also observed in regions where electrical coupling has not been well characterized, such as the amygdaloid nuclei. Where comparison was possible, the pattern of reporter in the brain was generally similar to that of Cx36 mRNA as assessed by in situ hybridization (Condorelli et al., 2000).

The number of cells expressing reporter in the neocortex and other brain regions at P15 is substantial. Possibly, some of the staining may represent gap junctions present only during neurogenesis and circuit formation, which are eliminated later in development (Connors et al., 1983; Yuste et al., 1992). Alternatively, the formation of electrical synapses containing Cx36 may be a relatively common feature of more mature GABAergic neurons. To explore the identity of the cells expressing reporter, 14 μM frozen sections were double labeled histochemically for β-gal and for either parvalbumin (PV; Figure 2B) or somatostatin (SS; Figure 2C) using antibodies. In previous studies, parvalbumin expression marked at least a subset of FS neurons but did not label

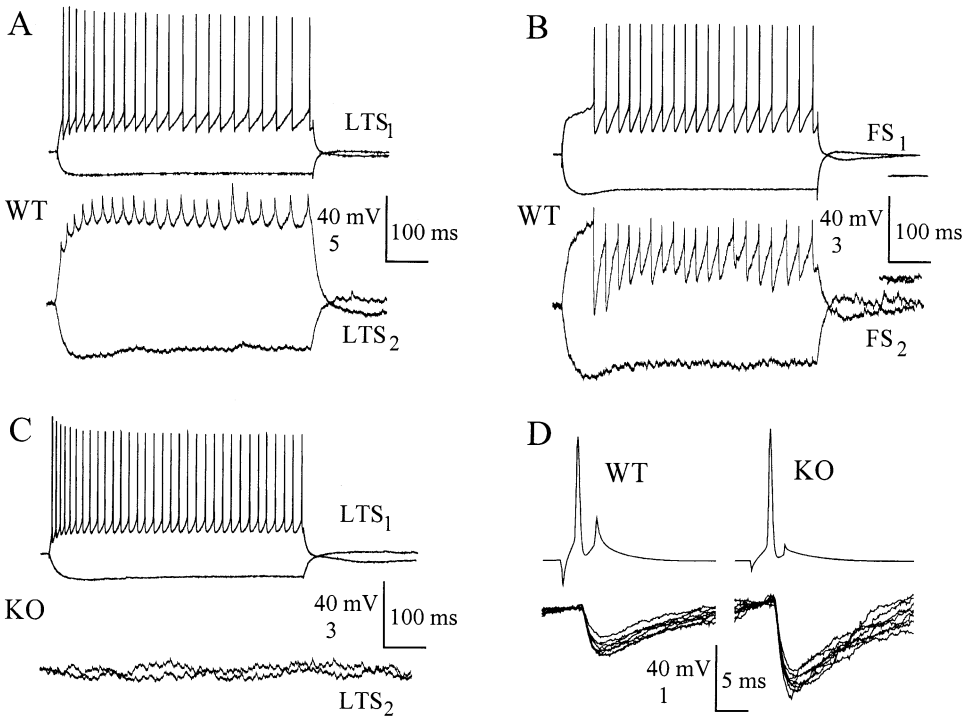

Figure 3. Electrical Coupling between Interneurons Is Rare and Weak in the KO

(A) Representative recordings showing coupling between a pair of LTS cells in WT neocortex. Note difference in voltage scale for driver and follower cells.

(B) Coupling between a pair of FS cells in WT; this pair also had an inhibitory chemical synapse, and spikes in FS_1 generated a series of compound electrical PSP-IPSPs in FS_2.

(C) Absence of coupling in a representative closely spaced pair of LTS cells from KO.

(D) Chemical inhibitory synapses in KO were similar to those in WT cortex (FS-FS cell pairs).

LTS neurons, while somatostatin expression displayed the opposite pattern (Gibson et al., 1999; Kawaguchi and Kubota, 1997).

In layer 4 of the barrel cortex, 78% of the β-gal-positive cells were also PV-positive (in 15 independent fields, 72 cells were positive only for β-gal, 140 were positive only for PV, and 239 cells were double positive). Conversely, 26% of β-gal-positive cells were also SS-positive (in 13 independent fields, 201 cells were positive only for β-gal, 141 were positive only for SS, and 54 were double positive; the micrographs in Figures 2B and 2C contain good examples of double labeled cells but are not numerically typical). Assuming no neurons are positive for both PV and SS, these findings are consistent with a restriction of Cx36 expression to PV- and SS-positive cells. However, significant numbers of PV-positive (37%) and SS-positive (73%) cells did not contain detectable β-gal reaction product. Thus, there could be a different ratio of Cx36-expressing cells in each class of interneuron. Analysis is complicated by the tendency of the histochemical and immunochemical signals to interfere with each other, and the problem that levels of both signal types varied significantly from cell to cell. While more quantitative results must await further study, it can be safely concluded that pyramidal cells do not widely express reporter but that many interneurons do.

Electrical Coupling Is Nearly Absent in the Knockout

Microelectrode recordings showed that the neocortex of the Cx36 knockout was dramatically deficient in electrical synapses. Electrical coupling was assessed by making paired whole-cell recordings from electrophysiologically identified neurons in layer 4 and passing current pulses sequentially into each cell (Figures 3A and 3B). As previously observed for rats (Gibson et al., 1999) electrical coupling occurred in more than 50% of wild-type pairs of similar interneurons (i.e., FS-FS or LTS-LTS), whereas pairs of dissimilar wild-type interneurons (FS-LTS) were not coupled (Table 1). Electrical coupling in knockout was rare and weak compared to wild-type (Figure 3C). Only 7% of sampled FS-FS pairs, and none of the LTS-LTS or FS-LTS pairs, had measurable electrical coupling in knockout (Table 1). Furthermore, the average coupling coefficient for the three coupled pairs of FS interneurons in knockout was only 10% that of the coupled wild-type pairs (Table 2).

Most other physiological properties of knockout interneurons were similar to those of wild-type interneurons (Table 2). The input resistances of FS and LTS neurons in the knockout were significantly higher than those of wild-type cells, but this would be expected if electrical synapses account for some of the input conductance

Table 1. Frequencies of Chemical and Electrical Synapses between Wild-Type (WT) and Knockout (KO) Neuron Pairs

Synaptic Connections Tested	Genotype	Total Cell Pairs	Electrical Synapses	Total Chemical Synapses	Reciprocal Chemical Synapses	Electrical and Chemical Synapses
FS↔FS	WT	21	12	27	11	12
	KO	30	3	38	14	3
LTS↔LTS	WT	5	3	0	0	0
	KO	3	0	0	0	0
LTS→FS	WT	10	0	6	4	0
	KO	14	0	6	5	0
FS→LTS	WT	10	0	5	4	0
	KO	14	0	8	5	0

Data include only cell pairs with somata spaced <70 μm apart. Arrows indicate the direction of chemical synaptic connection tested.

of each cell (Gibson et al., 1999). Spike frequency adaptation of FS cells (but not LTS cells) was slightly but significantly reduced in knockout neurons, perhaps as a consequence of the higher input resistances. Properties of the excitatory RS neurons in wild-type and knockout were indistinguishable. In addition to electrical synapses, FS cells frequently made inhibitory chemical synaptic connections with each other (Galarreta and Hestrin, 1999) and with LTS cells (Gibson et al., 1999; Tamas et al., 2000), whereas LTS cells formed chemical synapses with LTS cells but not FS cells (Gibson et al., 1999). The incidence, strength, and short-term plasticity of inhibitory postsynaptic potentials (IPSPs) were similar in wild-type and knockout (Figure 3D; Tables 1 and 2). We conclude that the major cellular phenotype of the Cx36 mutation is a dramatic reduction in the number and strength of electrical synapses among both FS and LTS interneurons.

ACPD Activates LTS Cells in Both WT and Knockout

If electrical synapses are critical for interneuron-based network synchrony, then synchrony in the Cx36 knockout should be severely compromised. We repeated experiments previously done in normal rat neocortex (Beierlein et al., 2000). The metabotropic glutamate receptor agonist ACPD caused nearly all LTS cells to depolarize and fire repetitive action potentials for the duration of the ACPD application, in both wild-type (30/33 cells) and knockout (15/16 cells) (Figure 4A). Prolonged excitation by ACPD was selective for LTS cells in wild-type and knockout; about 15% of FS cells (n = 80 wild-type, 92 knockout) were transiently (<10 s) depolarized above threshold by ACPD, and about 5% of FS cells generated sustained firing. When ACPD-activated LTS cells from wild-type were hyperpolarized with injected current, sharp subthreshold fluctuations of the membrane potential were often evident (18/35 cells; Figure 4B). In a previous study (Beierlein et al., 2000), these fluctuations were shown to be either attenuated, electrotonically conducted action potentials ("spikelets") or spike-independent oscillations from neighboring LTS cells. Despite being strongly depolarized by ACPD, LTS cells from knockout never generated such fluctuations (n = 17; Figure 4B). These observations are consistent with the absence of electrical synapses in our sample of LTS cell pairs from knockout.

Table 2. Electrophysiological Properties of Neurons and Inhibitory Synapses in Wild-Type (WT) and Knockout (KO)

		FS Cells	LTS Cells		RS Cells
Input resistance (MΩ)	WT	50 ± 20 (86)	108 ± 59 (38)		198 ± 70 (21)
	KO	66 ± 26 (108)[a]	153 ± 61 (22)[a]		172 ± 69 (25)
Spike width (ms)	WT	0.31 ± 0.07 (77)	0.57 ± 0.13 (36)		1.03 ± 0.24 (19)
	KO	0.31 ± 0.07 (82)	0.57 ± 0.13 (20)		0.99 ± 0.32 (20)
Frequency adaptation	WT	0.79 ± 0.19 (35)	0.58 ± 0.15 (29)		—
	KO	0.90 ± 0.16 (42)[a]	0.54 ± 0.15 (13)		—
Electrical coupling coefficient[b]	WT	0.061 ± 0.054 (11)	0.096 ± 0.045 (3)		—
	KO	0.006 ± 0.002 (3)[a]	—		—
IPSP amplitude (mV)	WT	2.0 ± 1.8 (21)[c]	0.5 ± 0.4 (6)[d]	1.5 ± 1.3 (5)[e]	—
	KO	1.5 ± 1.1 (35)[c]	1.0 ± 0.6 (5)[d]	2.0 ± 1.8 (5)[e]	—
IPSP dynamics	WT	0.50 ± 0.10 (15)[c]	1.0 ± 0.6 (6)[d]	0.5 ± 0.1 (5)[e]	—
	KO	0.47 ± 0.14 (35)[c]	1.0 ± 0.1 (4)[d]	0.4 ± 0.1 (4)[e]	—

Data are expressed as mean ± SD (number of cells or number of cell pairs for IPSP measurements). Input resistance was tested with small hyperpolarizing current pulses. Spike width of the last spike in train was measured at half amplitude. Spike frequency adaptation was calculated as (adapted/initial) frequencies (~220 Hz initial rate). IPSP dynamics measured as (average of last three IPSPs/first IPSP) amplitudes.

[a] $P < 0.01$ (Student's t test, two-tailed)

[b] Only cells with detectable coupling are included in these statistics.

[c] FS↔FS synapses

[d] LTS→FS synapses

[e] FS→LTS synapses

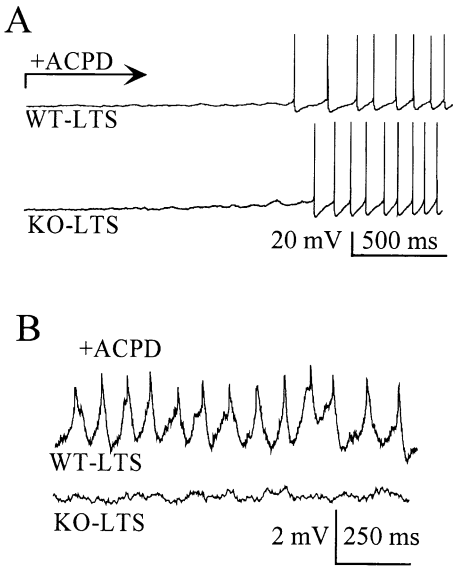

Figure 4. ACPD Excites LTS Cells Similarly in WT and KO

(A) ACPD depolarized and triggered spiking in LTS cells of both WT and KO.

(B) When activated by ACPD, WT-LTS cells held below the threshold for full action potentials displayed subthreshold spikelets; attenuated, they displayed electrotonically conducted action potentials. In contrast, LTS cells from the KO did not display spikelets.

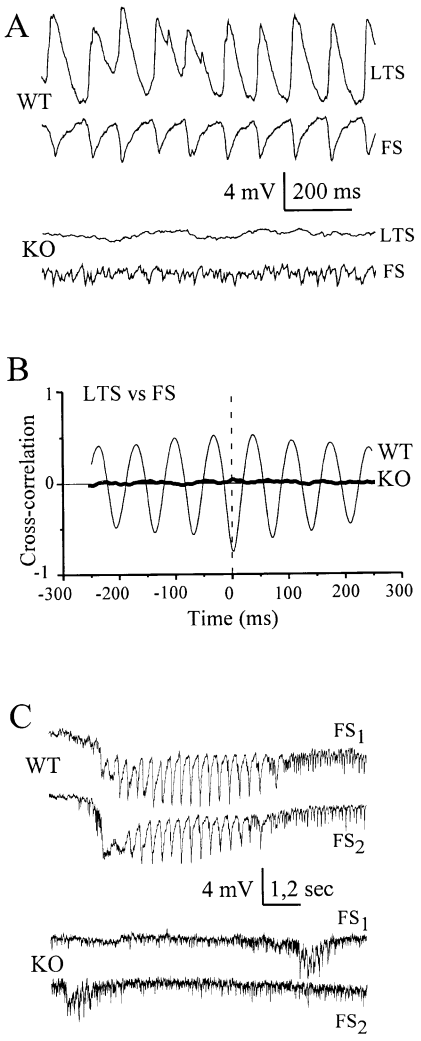

Figure 5. Correlation of Subthreshold ACPD-Induced LTS Fluctuations with IPSPs in Local FS Cells Is Lost in the KO

(A) In WT, simultaneous recordings showed rhythmic IPSPs in an FS cell, in phase with depolarizations in an LTS cell; LTS-FS pairs from KO generated more weakly correlated activity (distance between cells was 55 μm for the WT and 45 μm for the KO).

(B) Crosscorrelograms from cell pairs shown in (A); the LTS-FS pair from WT is strongly anticorrelated (thin trace) and has prominent side bands indicative of 14 Hz rhythmicity. LTS-FS pair from KO is nearly uncorrelated (thick trace).

(C) Epochs of 3–5 Hz ACPD-induced rhythmic IPSPs were highly correlated in a pair of FS cells from WT cortex (280 μm apart). ACPD-induced epochs of IPSPs from KO were uncorrelated and nonoverlapping (290 μm apart). One second time calibration applies to WT; 2 s calibration to KO.

Correlated Inhibition Is Reduced in the Knockout

In wild-type neocortex, ACPD-induced spiking in LTS cells coincided with repetitive IPSPs in local RS and FS cells (Beierlein et al., 2000). When LTS spiking was prevented with injected current, the subthreshold ACPD-induced fluctuations were highly anticorrelated with IPSPs in RS and FS cells (Figures 5A and 5B). Because spikelets never occurred in knockout LTS cells, strong correlations between the membrane activity of LTS and RS/FS cells were never observed in the knockout. The phase-locked activity induced by ACPD occurred at two distinct time scales. Younger cortex (P14–17) generated continuous, minutes-long rhythms at about 14 Hz (Figure 5A). When recorded as IPSPs in FS and RS cells, this relatively fast activity was larger in amplitude and more regular in wild-type as compared to knockout. Amplitudes of IPSPs recorded in FS and RS cells were measured as mean peak IPSP (wild-type = 2.0 ± 1.1mV, knockout = 1.3 ± 0.5mV [$p < 0.0005$]) or as the SD of the membrane fluctuations (wild-type = 0.62 ± 0.31mV, knockout = 0.42 ± 0.15mV [$p < 0.0003$]). Regularity was measured from 30 s traces that subjectively displayed the most consistent fast rhythmicity and had no clear 3–6 Hz epochs. First, power spectra were used to find the frequency (± 10% window) of maximum power. "Regularity" was defined as this power normalized by the total power from 1.5–70 Hz (expressed as percent). Regularity decreased with age in wild-type, from 35.7% ± 18.6% at P14–P17 to 18.6% ± 9.3% at >P17 ($p < 0.00003$; n = 35 and 22, respectively). Within the P14–P17 group, wild-type was more regular than knockout, although peak frequency was similar (power: 35.7% ± 18.6% for wild-type versus 22.2% ± 8.4% for knockout, $p < 0.001$; frequency: 13.4 ± 5.3 Hz for wild-type versus 14.1 ± 3.5 Hz for knockout, $p < 0.6$: n = 35 and 13).

ACPD also induced a more episodic activity at all ages (P14–21), typically consisting of 2–7 s epochs of rhythmic (3–5 Hz) or irregular fluctuations that repeated at about 0.07 Hz (Figure 5C). In FS and RS cells these epochs were generated by IPSPs; in LTS cells they were membrane fluctuations independent of chemical synapses (Beierlein et al., 2000). The incidence of ACPD-induced slower frequency IPSP epochs in FS and RS

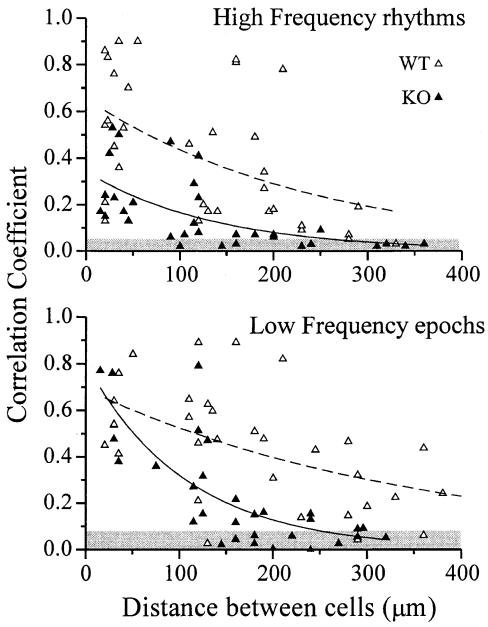

Figure 6. ACPD-Induced Synchrony Is Weaker and More Spatially Restricted in the KO

Scatter plot of normalized peak crosscorrelations as a function of intercellular distance. Each point represents a neuron pair; filled symbols are from KO, open symbols from WT. Gray zones show the baseline correlations derived from shuffled records. The top graph shows data from high-frequency (about 14 Hz) activity, from animals aged P14–17. The bottom graph shows low-frequency rhythmic activity from animals aged P14–21. Lines are the best-fits of single exponentials (dashed = WT, solid = KO). The high-frequency lines are significantly different in peak amplitude ($p < 0.001$); low-frequency lines have significantly different in space constants ($p < 0.001$) but have similar amplitudes at short distances.

cells was similar in the sample of wild-type (52%, n = 161) and knockout (47%, n = 155) cells, but IPSP amplitudes were larger in wild-type (3.5 ± 1.7mV, n = 70) than in knockout (2.9 ± 1.1mV, n = 71; $p < 0.02$), while the mean frequency was lower in wild-type (3.5 ± 0.7 Hz) than in knockout (5.2 ± 2.0 Hz, $p < 0.0000001$).

During both the faster (Figures 5A and 5B) and slower (Figure 5C) ACPD-induced activity, pairs of wild-type neurons were more strongly correlated than pairs of knockout neurons. Correlated activity was a steep function of intercellular distance, as assessed by recordings from neuron pairs with variable horizontal spacing (Figure 6) (Beierlein et al., 2000). Sustained high-frequency IPSPs were more strongly correlated in pairs of wild-type neurons than knockout neurons at all distances. Low-frequency IPSP epochs in wild-type and knockout cell pairs were similar at the shortest distances, but correlations fell much more steeply with distance in knockout than in wild-type. Correlations were at baseline levels for both high- and low-frequency epochs by about 200 μm in the knockout. The drop-off in correlation with distance in both wild-type and knockout is, in large part, due to epochs no longer occurring simultaneously over longer distances. We conclude that the amplitude, synchrony, and spatial extent of synchronous LTS-mediated activity were strongly impaired in the Cx36 knockout.

Discussion

Electrical coupling and spikelets were absent in LTS interneurons of knockout animals, and nearly all coupling was gone in FS cells of knockouts as well. We conclude that Cx36 is critical for the formation of functional gap junctions in most interneurons of the neocortex. The very small residual FS coupling suggests that other connexins may be present. It is possible that the constitutive deletion of Cx36 has resulted in a compensatory upregulation of other connexin genes. However, the majority of nonneural cells express multiple connexins (White and Paul, 1999), and it is likely that neurons do as well. In support of this idea, Cx32 transcript and protein have been reported in neurons (Micevych and Abelson, 1991; Nadarajah et al., 1997; Shiosaka et al., 1989), in one case together with Cx36 (Venance et al., 2000).

A most interesting characteristic of the Cx36 knockout was its severe impairment in the synchronous features of LTS-based rhythmic inhibition. This deficiency does not arise from an altered sensitivity of LTS cells to the metabotropic agonist, nor from an inability of the LTS cells to generate IPSPs in its FS and RS follower cells. Rather, it is likely that the absence of Cx36-based electrical synapses between LTS cells renders them incapable of coordinating their firing patterns. Uncorrelated firing within the LTS network precluded strongly synchronous inhibition across many neurons at long distances. Some modest and localized synchrony of IPSPs was maintained in the knockout, presumably because the axons of single LTS cells diverge onto common follower cells. Our results imply that electrical synapses serve to coordinate the activity patterns of large networks of inhibitory interneurons in neocortex. The wider generality of our conclusions is supported by similar findings in the hippocampus of a different Cx36 knockout mouse (H. Monyer, personal communication).

The Cx36 knockout mouse should prove valuable for understanding the functions of a variety of electrically coupled networks in the brain. Its cellular phenotype suggests that the knockout may suffer from abnormal electrographic rhythms of its forebrain circuits (Llinas et al., 1999). In this context, it is noteworthy that human Cx36 may be linked to a juvenile form of myoclonic epilepsy and an inherited abnormality in sensory responses associated with a predisposition to schizophrenia (Belluardo et al., 1999). FS cells have been implicated in sensory transformations of the neocortex (Azouz et al., 1997; Brumberg et al., 1996), and the possibility that their electrical synapses may coordinate the temporal or spatial characteristics of stimulus-mediated inhibition can be tested in the knockout. Finally, electrical synapses may critically influence other forms of synchrony. For example, in the developing retina, electrical synapses between ganglion and amacrine cells may influence the production of spontaneously arising waves of excitation (Catsicas et al., 1998; Roerig and Feller, 2000; Wong et al., 1998) which direct formation of eye-specific layers in the lateral geniculate nucleus (Katz and Shatz, 1996). A test of these ideas awaits the precise identification of the connexins expressed in these systems.

Experimental Procedures

Gene Targeting

Cx36 genomic clones were obtained from a 129SV genomic phage library (Stratagene) using a 533 bp probe corresponding to the sequences encoding the cytoplasmic loop and carboxy-terminus of Cx36. The probe was generated by PCR using primers A (GCGGAG GGAGCAAACGAGAAG) and B (CTGCCGAAATTGGGAACACTGAC). The targeting vector was based on pPNT (Tybulewicz et al., 1991) modified to incorporate a bicistronic reporter cassette containing *LacZ* (Shalaby et al., 1995) and IRES-*PLAP* (gift of C. Cepko). The construct was linearized at a unique SalI site adjacent to the TK and transfected into J1 ES cells that were selected for double resistance to G418 and gancyclovir. Resultant ES cell clones were screened by PCR with a 5′ primer external to the targeting vector (Primer C: ATTTGTTGCAGGGCAACTGAC) and a 3′ LacZ primer (Primer D: GCCTCTTCGCTATTACG). Six of 450 clones screened in this fashion showed correct recombination. After karyotyping, two lines were selected for injected into C57/B6 blastocysts resulting in germline-transmitting chimeras. Cx36 knockout progeny were genotyped by PCR using primer pair C and D to detect the targeted allele, and the primer pair A and B to detect the wild-type allele. 3′ homologous recombination was confirmed by PCR using the 5′ neoR primer (Primer E: TGTGCCCAGTCATAGCCGAATAGC) and a 3′ primer external to the targeting vector (Primer F: GATATGGTAGG TGGAGAGGAC). All experiments were performed on Cx36 knockout and wild-type littermates derived from F2 C57/B6-129SvEv mixed background litters. All mice were provided food and water ad lib and maintained in a constant 12 hr light:dark cycle prior to transport to Brown University for electrophysiological experiments.

Histochemistry and Immunocytochemistry

P14–20 Cx36 knockout and wild-type control littermate mice were deeply anesthetized with i.p. injection of Rompun/Ketaset (10–50 mg/ml). To obtain brains, animals were perfused with Ame's media (Sigma) followed by 4% paraformaldehyde in 1X Sorenson's buffer (pH 7.4), postfixed for 2 hr at room temperature after removal, and thoroughly washed in PBS. Retinas were obtained from perfused but unfixed animals. For histochemical detection of β-galactosidase activity, 100–200 μM vibratome sections were prepared as described (Agmon and Connors, 1991) and incubated at 37°C with 1mg/ml X-gal, 100 ng/ml NBT in 1X PBS, 2 mM $MgCl_2$, 2 mM EGTA for 1 to 4 hr. Sections were viewed using a dissecting microscope and transillumination. For immunocytochemistry, tissues were cryoprotected overnight in 30% sucrose, and 14 μm frozen sections were prepared and mounted on microscope slides. After the histochemical reaction, slides were washed thoroughly in PBS, blocked with 10% donkey serum, 2% BSA and incubated overnight with antibodies to parvalbumin (Sigma, 1:500) or somatostatin (Peninsula Labs, 1:1500). For somatostatin, blocking solution was supplemented with 0.1% Triton X-100. Primary antisera was detected using Vector ABC elite kit for labeling with HRP. For retina, anti-Cx36 antibody (Zymed) was used at 1/250 and detection utilized CY3-labeled secondary (Jackson Laboratories).

Electrophysiology

Cx36 knockout and wild-type control littermate mice from P14 to P21 were used. Preparation of thalamocortical slices, microelectrodes, recording apparatus, and pharmacologic agents were similar to those previously described (Beierlein et al., 2000) except that slices were 300–400 μm thick and microelectrodes contained 130 mM K-gluconate. Slices were maintained at 32°C. As described previously (Gibson et al., 1999), FS cells were distinguished by narrow action potentials (0.4–1 ms) each with a deep, brief afterhyperpolarization (AHP), the ability to generate high firing rates (up to 300 Hz), a long latency to the first spike near threshold, and little or no frequency adaptation. By contrast, LTS cells had broader spikes, pronounced frequency adaptation, never generated a long delay before spiking, and often displayed low-threshold spikes when depolarized from more negative resting potentials.

Experiments with ACPD were usually performed with 20 μM DNQX and 50 μM APV to block glutamate receptors, but this did not significantly change the results. The experimenter was blind to the genotype of the animals until after data were analyzed. Recordings were made from 129 wild-type and 124 knockout neuron pairs, of which 17 wild-type and 15 knockout neurons could not be reliably identified and were excluded from data presented here. Spike frequency adaptation was defined as the ratio of the final spiking rate to the initial spiking rate during 600 ms suprathreshold step current stimuli (Figures 3A and 3B). Average coupling coefficient was determined as previously described (Gibson et al., 1999). Short-term dynamics of inhibitory synapses were tested by evoking eight action potentials at 40 Hz in one cell while recording IPSPs in the other cell; dynamics are specified as the ratio of the final IPSP amplitude relative to the initial IPSP amplitude. Paired voltage records from ACPD experiments were analyzed with auto- and cross-correlograms and power spectra using Labview software (National Instruments) as previously described (Beierlein et al., 2000). Fast oscillation measurements were made on 30 s traces with no low frequency epochs. Correlations for low-frequency epochs were only done for pairs in which both cells displayed such epochs. The low-frequency correlation for each pair is the average correlation during each 2–7 s epoch that occurred in either cell. Baseline correlations were determined from randomly shuffled records of ACPD-induced activity.

Acknowledgments

We thank Hannah Monyer and her colleagues for sharing their results, Yael Amitai, Dan Goodenough, Michael Long, and David Pinto for comments on the manuscript, and Saundra Patrick for excellent technical assistance. This study was supported by National Institutes of Health grants GM37751, GM18974, NS25983, and DA12500.

Received April 5, 2001; revised June 6, 2001.

References

Agmon, A., and Connors, B.W. (1991). Thalamocortical responses of mouse somatosensory (barrel) cortex in vitro. Neuroscience *41*, 365–379.

Azouz, R., Gray, C.M., Nowak, L.G., and McCormick, D.A. (1997). Physiological properties of inhibitory interneurons in cat striate cortex. Cereb. Cortex *7*, 534–545.

Beierlein, M., Gibson, J.R., and Connors, B.W. (2000). A network of electrically coupled interneurons drives synchronized inhibition in neocortex. Nat. Neurosci. *3*, 904–910.

Belluardo, N., Trovato-Salinaro, A., Mudo, G., Hurd, Y.L., and Condorelli, D.F. (1999). Structure, chromosomal localization, and brain expression of human Cx36 gene. J. Neurosci. Res. *57*, 740–752.

Benardo, L.S. (1997). Recruitment of GABAergic inhibition and synchronization of inhibitory interneurons in rat neocortex. J. Neurophysiol. *77*, 3134–3144.

Bennett, M.V. (1997). Gap junctions as electrical synapses. J. Neurocytol. *26*, 349–366.

Bragin, A., Jando, G., Nadasdy, Z., Hetke, J., Wise, K., and Buzsaki, G. (1995). Gamma (40–100 Hz) oscillation in the hippocampus of the behaving rat. J. Neurosci. *15*, 47–60.

Brumberg, J.C., Pinto, D.J., and Simons, D.J. (1996). Spatial gradients and inhibitory summation in the rat whisker barrel system. J. Neurophysiol. *76*, 130–140.

Buzsaki, G., and Chrobak, J.J. (1995). Temporal structure in spatially organized neuronal ensembles: a role for interneuronal networks. Curr. Opin. Neurobiol. *5*, 504–510.

Catsicas, M., Bonness, V., Becker, D., and Mobbs, P. (1998). Spontaneous Ca2+ transients and their transmission in the developing chick retina. Curr. Biol. *8*, 283–286.

Condorelli, D.F., Belluardo, N., Trovato-Salinaro, A., and Mudo, G. (2000). Expression of Cx36 in mammalian neurons. Brain Res. Brain Res. Rev. *32*, 72–85.

Connors, B.W., Benardo, L.S., and Prince, D.A. (1983). Coupling between neurons of the developing rat neocortex. J. Neurosci. *3*, 773–782.

Galarreta, M., and Hestrin, S. (1999). A network of fast-spiking cells in the neocortex connected by electrical synapses. Nature *402*, 72–75.

Gibson, J.R., Beierlein, M., and Connors, B.W. (1999). Two networks of electrically coupled inhibitory neurons in neocortex. Nature *402*, 75–79.

Jefferys, J.G., Traub, R.D., and Whittington, M.A. (1996). Neuronal networks for induced '40 Hz' rhythms. Trends Neurosci. *19*, 202–208.

Katz, L.C., and Shatz, C.J. (1996). Synaptic activity and the construction of cortical circuits. Science *274*, 1133–1138.

Kawaguchi, Y., and Kubota, Y. (1997). GABAergic cell subtypes and their synaptic connections in rat frontal cortex. Cereb. Cortex *7*, 476–486.

Llinas, R.R., Ribary, U., Jeanmonod, D., Kronberg, E., and Mitra, P.P. (1999). Thalamocortical dysrhythmia: A neurological and neuropsychiatric syndrome characterized by magnetoencephalography. Proc. Natl. Acad. Sci. USA *96*, 15222–15227.

Lytton, W.W., and Sejnowski, T.J. (1991). Simulations of cortical pyramidal neurons synchronized by inhibitory interneurons. J. Neurophysiol. *66*, 1059–1079.

Micevych, P.E., and Abelson, L. (1991). Distribution of mRNAs coding for liver and heart gap junction proteins in the rat central nervous system. J. Comp. Neurol. *305*, 96–118.

Michelson, H.B., and Wong, R.K. (1994). Synchronization of inhibitory neurones in the guinea-pig hippocampus in vitro. J. Physiol. *477 (Pt 1)*, 35–45.

Nadarajah, B., Jones, A.M., Evans, W.H., and Parnavelas, J.G. (1997). Differential expression of connexins during neocortical development and neuronal circuit formation. J. Neurosci. *17*, 3096–3111.

Rash, J.E., Staines, W.A., Yasumura, T., Patel, D., Furman, C.S., Stelmack, G.L., and Nagy, J.I. (2000). Immunogold evidence that neuronal gap junctions in adult rat brain and spinal cord contain connexin-36 but not connexin-32 or connexin-43. Proc. Natl. Acad. Sci. USA *97*, 7573–7578.

Raviola, E., and Gilula, N.B. (1975). Intramembrane organization of specialized contacts in the outer plexiform layer of the retina. A freeze-fracture study in monkeys and rabbits. J. Cell Biol. *65*, 192–222.

Raviola, E., and Raviola, G. (1982). Structure of the synaptic membranes in the inner plexiform layer of the retina: a freeze-fracture study in monkeys and rabbits. J. Comp. Neurol. *209*, 233–248.

Roerig, B., and Feller, M.B. (2000). Neurotransmitters and gap junctions in developing neural circuits. Brain Res. Brain Res. Rev. *32*, 86–114.

Shalaby, F., Rossant, J., Yamaguchi, T.P., Gertsenstein, M., Wu, X.F., Breitman, M.L., and Schuh, A.C. (1995). Failure of blood-island formation and vasculogenesis in Flk-1-deficient mice. Nature *376*, 62–66.

Shiosaka, S., Yamamoto, T., Hertzberg, E.L., and Nagy, J.I. (1989). Gap junction protein in rat hippocampus: correlative light and electron microscope immunohistochemical localization. J. Comp. Neurol. *281*, 282–297.

Sohl, G., Degen, J., Teubner, B., and Willecke, K. (1998). The murine gap junction gene connexin36 is highly expressed in mouse retina and regulated during brain development. FEBS Lett. *428*, 27–31.

Steriade, M. (1997). Synchronized activities of coupled oscillators in the cerebral cortex and thalamus at different levels of vigilance. Cereb. Cortex *7*, 583–604.

Swadlow, H.A., Beloozerova, I.N., and Sirota, M.G. (1998). Sharp, local synchrony among putative feed-forward inhibitory interneurons of rabbit somatosensory cortex. J. Neurophysiol. *79*, 567–582.

Tamas, G., Buhl, E.H., Lorincz, A., and Somogyi, P. (2000). Proximally targeted GABAergic synapses and gap junctions synchronize cortical interneurons. Nat. Neurosci. *3*, 366–371.

Tybulewicz, V.L., Crawford, C.E., Jackson, P.K., Bronson, R.T., and Mulligan, R.C. (1991). Neonatal lethality and lymphopenia in mice with a homozygous disruption of the c-abl proto-oncogene. Cell *65*, 1153–1163.

Venance, L., Rozov, A., Blatow, M., Burnashev, N., Feldmeyer, D., and Monyer, H. (2000). Connexin expression in electrically coupled postnatal rat brain neurons. Proc. Natl. Acad. Sci. USA *97*, 10260–10265.

White, T.W., and Paul, D.L. (1999). Genetic diseases and gene knockouts reveal diverse connexin functions. Annu. Rev. Physiol. *61* 283–310.

Whittington, M.A., Traub, R.D., and Jefferys, J.G. (1995). Synchronized oscillations in interneuron networks driven by metabotropic glutamate receptor activation. Nature *373*, 612–615.

Wong, W.T., Sanes, J.R., and Wong, R.O. (1998). Developmentally regulated spontaneous activity in the embryonic chick retina. J. Neurosci. *18*, 8839–8852.

Yuste, R., Peinado, A., and Katz, L.C. (1992). Neuronal domains in developing neocortex. Science *257*, 665–668.